

Full length article

# Temperature-dependent dielectric functions and interband critical points of sulfur-rich $\text{TlIn}(\text{S}_{1-x}\text{Se}_x)_2$ layered solid solution crystals



O.O. Gomonnai<sup>a,\*</sup>, O. Gordan<sup>b</sup>, P.P. Guranich<sup>a</sup>, A.G. Slivka<sup>a</sup>, A.V. Gomonnai<sup>a,c</sup>,  
D.R.T. Zahn<sup>b</sup>

<sup>a</sup> Uzhhorod National University, 46 Pidhirna Str., 88000 Uzhhorod, Ukraine

<sup>b</sup> Semiconductor Physics, Technische Universität Chemnitz, D-09107 Chemnitz, Germany

<sup>c</sup> Institute of Electron Physics, Ukr. Nat. Acad. Sci., 21 Universytetska Str., 88017 Uzhhorod, Ukraine

## ARTICLE INFO

## Article history:

Received 10 December 2016

Received in revised form 21 January 2017

Accepted 22 January 2017

Available online 24 January 2017

## Keywords:

Dielectric function

Optical transitions

Structural phase transitions

## ABSTRACT

Real and imaginary parts of the dielectric function of  $\text{TlIn}(\text{S}_{1-x}\text{Se}_x)_2$  ( $x=0.05, 0.08, 0.25$ ) single crystals were determined in the spectral range from 1 to 5 eV within a temperature interval 140–293 K from spectroscopic ellipsometry measurements. The energies of interband transitions (critical points) of the  $\text{TlIn}(\text{S}_{1-x}\text{Se}_x)_2$  crystals were obtained from the second derivative of the real and imaginary parts of dielectric function. Structural phase transitions are behind the observed change of electronic band structure.

© 2017 Elsevier B.V. All rights reserved.

## 1. Introduction

Layered ferroelectrics are interesting for investigation since their properties are determined by the quasi-two-dimensionality and a strong structural anisotropy [1]. This class of materials includes  $\text{TlInS}_2$  which is especially interesting since it possesses a complex sequence of phase transitions (PTs) in the temperature interval of 190–216 K [2–14] and polycritical phenomena in the ( $p, T$ )-phase diagram in the pressure range of  $580 \leq p \leq 660$  MPa [15–19].  $\text{TlInS}_2$  and  $\text{TlInSe}_2$  compounds give rise to a series of  $\text{TlIn}(\text{S}_{1-x}\text{Se}_x)_2$  mixed crystals where for a Se concentration of about 0.7–0.75 the crystal structure changes from  $C_{2h}^6$  to  $D_{4h}^{18}$  symmetry [20–23]. Note that only quite a few studies using X-ray diffraction [20,21], Raman scattering and infrared reflection spectroscopy [24–29], transmission and reflection spectroscopy in the wavelength range of 400–1100 nm [30,31], and dielectric measurements [23,32,33] of the  $\text{TlIn}(\text{S}_{1-x}\text{Se}_x)_2$  mixed crystal system were reported. However, most of the studies were performed for a series of samples with a rather limited number of compositions within the whole  $x$  interval. In Refs. 23–26 and 33 particular attention was paid to sulphur-rich  $\text{TlIn}(\text{S}_{1-x}\text{Se}_x)_2$  crystals and with  $x \leq 0.2$ .

The temperature behaviour of the dielectric constant ( $10^3$ – $10^6$  Hz) in sulphur-rich  $\text{TlIn}(\text{S}_{1-x}\text{Se}_x)_2$  mixed crystals in the temperature interval including the phase transition range was reported earlier [23,32,33]. It was shown there that isovalent anionic substitution of S by Se leads to a downward shift of the structural phase transition temperatures with a simultaneous shrinking of the temperature interval of the incommensurate phase existence. It was concluded that in the ( $x, T$ ) phase diagram of the  $\text{TlIn}(\text{S}_{1-x}\text{Se}_x)_2$  crystals a Lifshitz type point can exist at  $x=0.05$  [23] similarly to another chalcogenide ferroelectric solid solution system  $\text{Sn}_2\text{P}_2(\text{S}_{1-x}\text{Se}_x)_6$  [34]. However, other authors report contradictory data with respect to the phase transitions in  $\text{TlIn}(\text{S}_{1-x}\text{Se}_x)_2$  solid solutions: the PT temperatures  $T_i = 232$  K,  $T_{c1} = 216$  K, and  $T_{c2} = 212$  K for  $\text{TlInS}_2$ , while substitution of S by Se shifts the PTs down to  $T_i = 210$  K,  $T_{c1} = 200$  K, and  $T_{c2} = 196.8$  K for  $\text{TlInSe}_2$  [32].

This, in our opinion, increases the interest towards the investigation of sulphur-rich  $\text{TlIn}(\text{S}_{1-x}\text{Se}_x)_2$  mixed crystals.

Ellipsometric studies of  $\text{TlInS}_2$ -type chalcogenides were carried out earlier [35–41]. In particular, interband transitions for  $\text{TlGaS}_2$  [35,36,40],  $\text{TlGaSe}_2$  [35], and  $\text{TlInS}_2$  [35,39,41] crystals were determined. Second derivative spectra of the dielectric function were analysed for  $\text{TlGaS}_2\text{Se}_{2(1-x)}$  [37] and  $\text{TlGa}_x\text{In}_{1-x}\text{S}_2$  solid solutions [38]. Meanwhile, for  $\text{TlInS}_2\text{Se}_{2(1-x)}$  such analysis was performed only for the crystals with  $x = 0.25, 0.5$ , and  $0.75$  at room temperature [39].

\* Corresponding author.

E-mail address: [gomonnai.o@gmail.com](mailto:gomonnai.o@gmail.com) (O.O. Gomonnai).

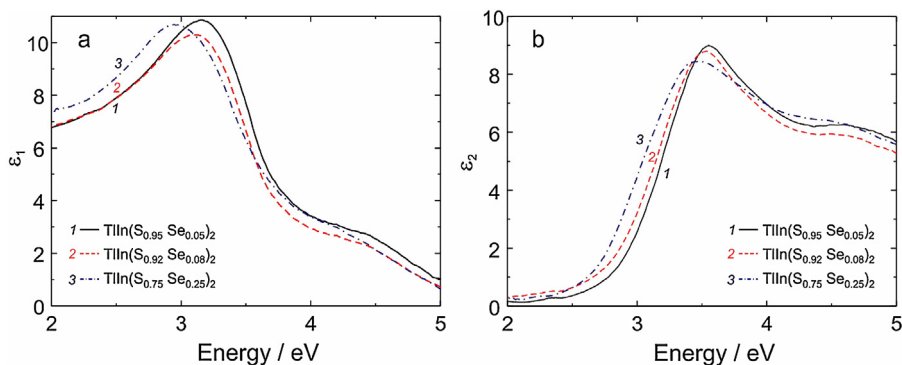


**Fig. 1.** Spectra of the real (a) and imaginary (b) part of the complex dielectric function of  $\text{TlIn}(\text{S}_{1-x}\text{Se}_x)_2$  ( $x=0.05, 0.08, 0.25$ ) crystals obtained from the ellipsometry measurements performed at room temperature.

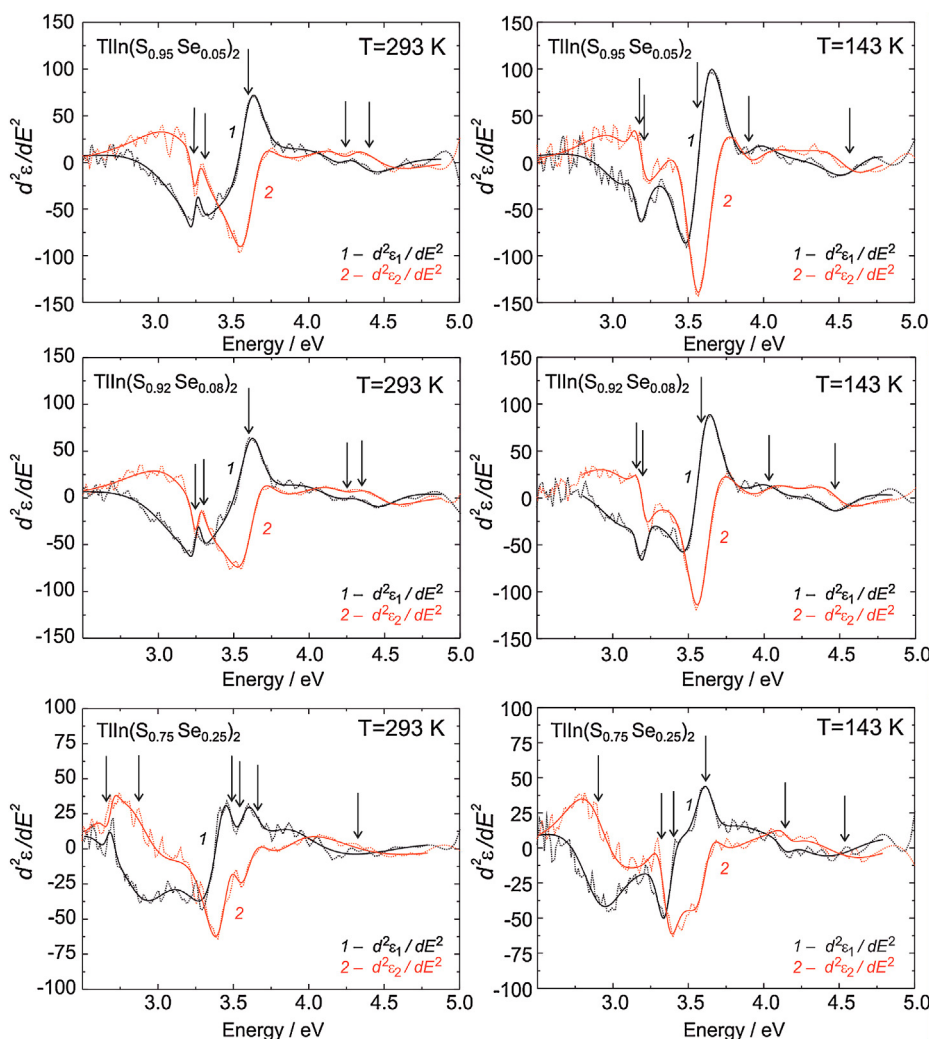


**Fig. 2.** Second energy derivative spectra of the dielectric function for  $\text{TlIn}(\text{S}_{1-x}\text{Se}_x)_2$  ( $x=0.05, 0.08, 0.25$ ) crystals at  $T=293$  K (a) and  $T=143$  K (b). Dotted curves show the experimental data. Solid lines represent fitting of the second-energy derivative spectra of the real and imaginary parts of the dielectric function, respectively. Arrows indicate the energies of the critical points.

In this study, we present the temperature behaviour of the dielectric function of sulphur-rich  $\text{TlIn}(\text{S}_{1-x}\text{Se}_x)_2$  crystals from 140 to 293 K in the 1–5 eV photon energy range. The critical points (CPs) for interband optical transitions were derived from the dielectric function spectra. Based on the temperature behaviour of the dielectric function and the CPs, we discuss the effect of the structural

phase transitions on the electronic band structure in sulphur-rich  $\text{TlIn}(\text{S}_{1-x}\text{Se}_x)_2$  crystals.

## 2. Experimental

$\text{TlIn}(\text{S}_{1-x}\text{Se}_x)_2$  ( $x=0, 0.05, 0.08, 0.25$ ) single crystals were grown by the Bridgman technique, the details and characteristics being

**Table 1**  
Critical point energies for sulphur-rich  $\text{TlIn}(\text{S}_{1-x}\text{Se}_x)_2$  crystals.

	$E_{c1}$ (eV)	$E_{c2}$ (eV)	$E_{c3}$ (eV)	$E_{c4}$ (eV)	$E_{c5}$ (eV)	$E_{c6}$ (eV)
$\text{TlIn}(\text{S}_{0.95}\text{Se}_{0.05})_2$	$3.24 \pm 0.01$	$3.32 \pm 0.02$	$3.60 \pm 0.01$	$4.25 \pm 0.10$	$4.39 \pm 0.10$	
$\text{TlIn}(\text{S}_{0.92}\text{Se}_{0.08})_2$	$3.25 \pm 0.01$	$3.30 \pm 0.02$	$3.61 \pm 0.01$	$4.27 \pm 0.30$	$4.36 \pm 0.30$	
$\text{TlIn}(\text{S}_{0.75}\text{Se}_{0.25})_2$	$2.68 \pm 0.01$	$2.88 \pm 0.05$	$3.49 \pm 0.30$	$3.51 \pm 0.30$	$3.65 \pm 0.20$	$4.31 \pm 0.20$

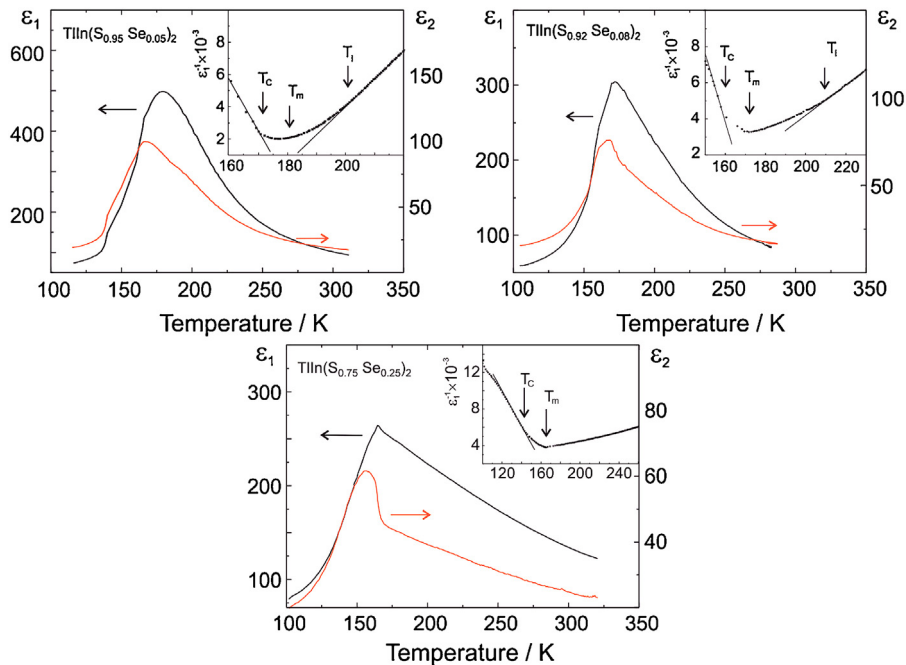


**Fig. 3.** Temperature dependences of the real and imaginary parts of the complex dielectric function and  $\varepsilon_1^{-1}(T)$  of  $\text{TlIn}(\text{S}_{1-x}\text{Se}_x)_2$  ( $x = 0.05, 0.08,$  and  $0.25$ ) measured at 1 MHz. The inset shows the  $\varepsilon_1^{-1}(T)$  plot.

described elsewhere [42]. The crystal quality and chemical composition were checked by surface imaging using scanning electron microscopy with local elemental analysis by energy-dispersive X-ray fluorescence spectroscopy, Raman spectroscopy, and X-ray diffraction studies [42]. The results obtained for the samples under investigation agree well with the data for the  $C_{2h}^6$  space group, typical for  $\text{TlInS}_2$  crystals at room temperature and atmospheric pressure and described in the literature as a stable structure [1].

The dielectric constant was measured at a frequency of 1 MHz using an ac bridge with a temperature rate of 0.01–0.02 K/s. Samples with the size of  $4 \times 4 \times 2 \text{ mm}^3$  were used for the measurements. Contacts were applied using silver conductive paste.

Spectroscopic ellipsometry measurements were carried out using a Variable Angle Spectroscopic Ellipsometer J.A. from Woolam Co., Inc. The angle of the incident light beam was adjusted to  $70^\circ$ . The measurements were performed for up to 3 mm thick samples, the flat (001) surface area of up to  $10 \times 10 \text{ mm}^2$  being perpendicular to the optic axis  $\mathbf{c}$ . The real ( $\varepsilon_1$ ) and imaginary ( $\varepsilon_2$ ) parts of the effective dielectric function of the  $\text{TlIn}(\text{S}_{1-x}\text{Se}_x)_2$  single crystals were obtained in the spectral range of 1–5 eV. The measurements were performed in the temperature range 140–293 K using a Linkam THMS600 stage.

### 3. Results and discussion

We performed spectroscopic ellipsometry measurements for the above series of  $\text{TlIn}(\text{S}_{1-x}\text{Se}_x)_2$  single crystals. The corresponding data represent changes in the polarization state undergone by the incident linearly polarized light beam when it is reflected by the sample surface. This change is expressed as the ratio between

the complex reflection coefficients for the polarization parallel ( $r_p$ ) and perpendicular ( $r_s$ ) to the plane of incidence. The spectroscopic measurements are given in terms of the ellipsometric angles  $\psi$  and  $\Delta$  as functions of the photon energy. Thus, construction of a physical model for the  $r_p$  and  $r_s$  coefficients enables several parameters to be determined by fitting the spectra calculated using Eq. (1) to the experimental measurements [43]

$$\rho = \frac{r_p}{r_s} = \tan(\psi) \exp(i\Delta) \quad (1)$$

The dielectric functions of crystals, thin films, and other materials are obtained using different theoretical optical models. A simple ambient-substrate optical model was used to find the dielectric function of bulk flat crystals expressed as [43]

$$\varepsilon = \varepsilon_1 + i\varepsilon_2 = \sin^2(\phi) \left[ 1 + \left( \frac{1-\rho}{1+\rho} \right)^2 \tan^2(\phi) \right] \quad (2)$$

where  $\phi$  is the angle of incidence.

Spectral dependences of the dielectric function of  $\text{TlIn}(\text{S}_{1-x}\text{Se}_x)_2$  ( $x = 0.05, 0.08, 0.25$ ) solid solutions at room temperature are shown in Fig. 1. As one can see from the figures, an increasing Se content results in the spectrum shift towards lower energies which is in agreement with the earlier data [39].

Detailed information about the energies of the interband transitions (critical points) for  $\text{TlIn}(\text{S}_{1-x}\text{Se}_x)_2$  crystals can be obtained from the analysis of the dielectric function. The critical point analysis can be performed using the second derivative spectra of the

dielectric function. The corresponding theoretical expression is given by [43,44]:

$$\frac{d^2 \varepsilon}{dE^2} = m(m-1)A \exp(i\varphi) (E - E_g + i\Gamma)^{m-2} \quad m \neq 0 \quad (3)$$

$$\frac{d^2 \varepsilon}{dE^2} = A \exp(i\varphi) (E - E_g + i\Gamma)^{-2} \quad (m = 0)$$

where  $E$  is energy,  $A$  is the amplitude,  $E_{cp}$  is the critical point energy,  $\Gamma$  is the broadening parameter,  $\varphi$  is the phase angle, and  $m$  is related to the dimensions of wave vectors taking part in the optical transitions. Each critical point is classified into one, two, and three dimensions with actual  $m$  values equal to  $-1/2$ ,  $0$ , and  $+1/2$  for one-, two-, and three-dimensional cases, respectively [43]. Furthermore, when an optical transition exhibits excitonic behaviour,  $m = -1$  [43].

The dielectric function of the three different  $\text{TlIn}(\text{S}_{1-x}\text{Se}_x)_2$  compositions ( $x=0.05, 0.08, \text{ and } 0.25$ ) was studied based on the ellipsometry measurements performed at different temperatures decreasing from 293 to 143 K with a step of 10 K. The second derivative spectra of the dielectric function in the energy range 2.5–5 eV for  $T=293$  K and  $T=143$  K obtained from those shown in Fig. 1 using the procedure described below are shown in Fig. 2.

Smoothing was performed using Savitzky–Golay filtering method [45]. The function (3) was introduced in the analytic software with the parameter  $m = -1$ . The calculation was performed simultaneously for the real  $\varepsilon_1$  and imaginary  $\varepsilon_2$  parts of dielectric function by Levenberg–Marquardt algorithm to adjust the parameter values in the iterative procedure. The accuracy of the results obtained is characterized by a coefficient of determination  $R^2$  which was above 0.96 for all the temperatures under investigation.

At the beginning we introduced initial  $E_{cp}$  values which were subsequently automatically corrected in the fitting process. The fitting procedure was performed for different number of critical points. The output calculation parameters (critical point energy  $E_{cp}$ , amplitude  $A$ , broadening  $\Gamma$ , and phase angle  $\varphi$ ) were adjusted until the tolerance value  $\chi^2$  of  $1 \times 10^{-9}$  was reached.

The analysis of the second derivative spectra of the dielectric function at room temperature in the above-bandgap region revealed the presence of five critical points for  $\text{TlIn}(\text{S}_{0.95}\text{Se}_{0.05})_2$ , and  $\text{TlIn}(\text{S}_{0.92}\text{Se}_{0.08})_2$  as well as six critical points for  $\text{TlIn}(\text{S}_{0.75}\text{Se}_{0.25})_2$  listed in Table 1.

Analysis of the temperature dependences of the changes of the dielectric function second derivative spectra requires information on the compositional dependence of the phase transition temperatures for the  $\text{TlIn}(\text{S}_{1-x}\text{Se}_x)_2$  solid solutions under investigation. We obtained these data from the experimental measurements of the temperature dependence of the dielectric constant (real  $\varepsilon_1(T)$  and imaginary  $\varepsilon_2(T)$  parts) performed at 1 MHz.

The temperature dependences of the real  $\varepsilon_1(T)$  and imaginary  $\varepsilon_2(T)$  parts of the dielectric constant for  $\text{TlIn}(\text{S}_{1-x}\text{Se}_x)_2$  with  $x=0.05, 0.08, \text{ and } 0.25$  are shown in Fig. 3. Similarly to Ref. [23], we plotted  $\varepsilon_1^{-1}(T)$  dependences for  $\text{TlIn}(\text{S}_{1-x}\text{Se}_x)_2$  (the inset in Fig. 3) where one can observe anomalies at  $T_i$ ,  $T_c$ , and  $T_m$ . The first two values correspond to the phase transitions from the paraelectric to the incommensurate phase ( $T_i$ ) and from the incommensurate to the paraelectric phase ( $T_c$ ) while  $T_m$  is the temperature value corresponding to the  $\varepsilon$  maximum.

For  $\text{TlIn}(\text{S}_{0.95}\text{Se}_{0.05})_2$  the anomalies in  $\varepsilon_1^{-1}(T)$  are observed at  $T_c = 170$  K,  $T_m = 182$  K, and  $T_i = 203$  K, for  $\text{TlIn}(\text{S}_{0.92}\text{Se}_{0.08})_2$  the corresponding values are  $T_c = 160$  K,  $T_m = 172$  K, and  $T_i = 205$  K while for  $\text{TlIn}(\text{S}_{0.75}\text{Se}_{0.25})_2$   $T_c = 144$  K,  $T_m = 162$  K (no anomaly ascribed to  $T_i$  was observed in the  $\varepsilon_1(T)$  and  $\varepsilon_2(T)$  for  $x=0.25$ ). One should note that the PT temperature  $T_c = 168$  K reported for  $\text{TlIn}(\text{S}_{0.95}\text{Se}_{0.05})_2$  in a recent study [23] is in agreement with the present data. The increase of the selenium content in  $\text{TlIn}(\text{S}_{1-x}\text{Se}_x)_2$  crystals in gen-

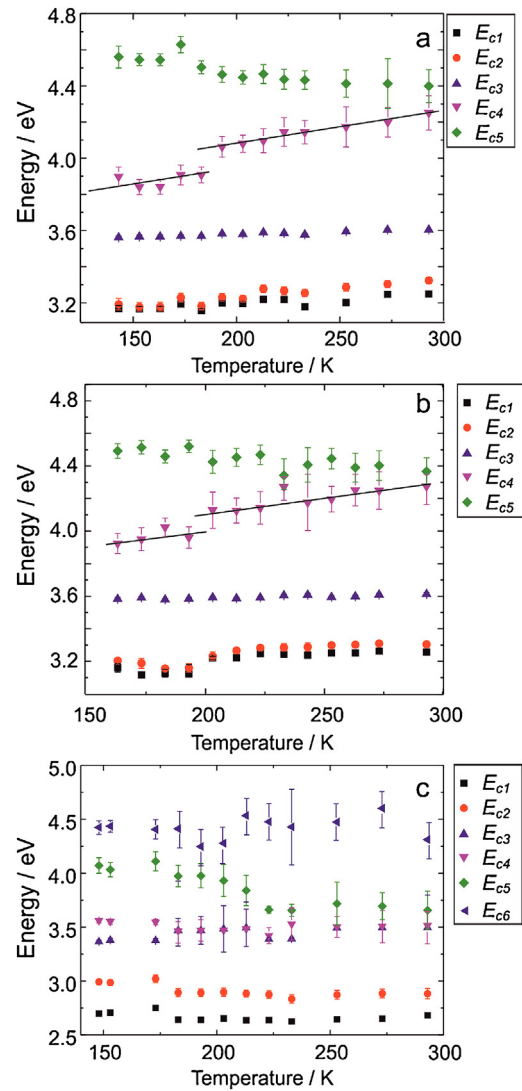


Fig. 4. Temperature dependences of interband critical points energies  $E_c$  for  $\text{TlIn}(\text{S}_{1-x}\text{Se}_x)_2$  with  $x=0.05$  (a),  $0.08$  (b),  $0.25$  (c).

eral results in a decrease of the dielectric constant and a shift of the anomalies towards lower temperatures. Note that a slight increase of  $T_i$  is observed for  $\text{TlIn}(\text{S}_{0.92}\text{Se}_{0.08})_2$ .

For  $\text{TlIn}(\text{S}_{0.95}\text{Se}_{0.05})_2$  the critical point energies  $E_{c1}$  and  $E_{c2}$  decrease with decreasing temperature from 293 to 143 K while  $E_{c3}$  remains practically unchanged and  $E_{c5}$  gradually increases; meanwhile,  $E_{c4}$  decreases down to 4.06 eV at  $T = 193$  K when a stepwise drop to 3.90 eV is observed with only slight fluctuations at subsequent cooling down to 143 K (See Fig. 4a). The observed anomaly of  $E_{c4}$  at 193 K correlates with the phase transition temperature  $T_i$  (Fig. 3).

As can be seen from Fig. 4b, for the  $\text{TlIn}(\text{S}_{0.92}\text{Se}_{0.08})_2$  CPs the following temperature behaviour is observed: the  $E_{c1}$  and  $E_{c2}$  energies decrease with cooling while  $E_{c3}$  remains almost unchanged and  $E_{c2}$  increases. The  $E_{c4}$  behaviour is similar to that for  $\text{TlIn}(\text{S}_{0.95}\text{Se}_{0.05})_2$ :  $E_{c4}$  decreases with cooling with a stepwise drop, which is observed at a somewhat higher temperature  $T = 203$  K which correlates with the temperature  $T_i$  of the crystal transition to the incommensurate phase (Fig. 3).

The dielectric function second energy derivative spectra of  $\text{TlIn}(\text{S}_{0.75}\text{Se}_{0.25})_2$  are well described by six critical points at low temperatures (up to 173 K). Note that the same number of CPs was reported for this crystal from room-temperature studies [39].

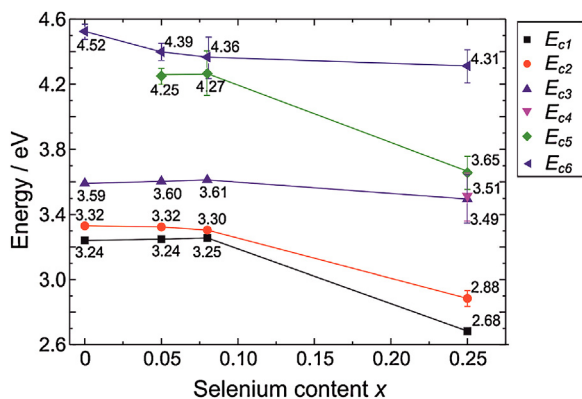


**Fig. 5.** Dependence of critical point energies on the  $\text{TlIn}(\text{S}_{1-x}\text{Se}_x)_2$  mixed crystal composition at room temperature. For the points where the error bars are not shown explicitly, they are smaller than the corresponding symbol signs.

However, as follows from our study, at  $T \geq 183$  K the spectra can be sufficiently well described using five CPs (Fig. 4c). The  $E_{c1}$  and  $E_{c2}$  values remain practically unchanged with cooling, exhibiting only a slight increase near 173 K. With cooling down to 148 K the CP with an energy near 3.5 eV does not shift either; however, at lower temperatures one can distinguish two CPs in this energy range, namely  $E_{c3}$  and  $E_{c4}$ . The  $E_{c5}$  value remains almost the same at cooling until 223 K (3.66 eV) when it begins to increase up to 4.07 eV at  $T = 148$  K. The  $E_{c6}$  energy position does not reveal any noticeable trend with cooling, being characterized by noticeable fluctuations and higher determination error.

The  $E_{c5}$  transformation near 173 K in the above plot is basically in agreement with the dependences based on the data for the ac bridge measurements where a maximum in the vicinity of the  $T_m$  temperature is observed (see Fig. 3). Further studies are required to explain the  $E_{c5}$  transformation at 223 K.

Recently, the analysis of phase transformations based on the ellipsometry data was performed for  $\text{TlGaS}_2$  [40] where kinks were observed in the  $E_{cp}(T)$  dependences which, in the authors' opinion, correspond to structural PTs.

The compositional behaviour of the critical point energies for  $\text{TlIn}(\text{S}_{1-x}\text{Se}_x)_2$  single crystals ( $0 \leq x \leq 0.25$ ) is shown in Fig. 5.

#### 4. Conclusions

The real and imaginary parts of the dielectric function in the spectral range 1–5 eV were found for  $\text{TlIn}(\text{S}_{1-x}\text{Se}_x)_2$  ( $x = 0.05, 0.08, 0.25$ ) crystals at temperatures in the range of 140–293 K based on spectroscopic ellipsometry measurements. The energies of inter-band transitions (critical points) for  $\text{TlIn}(\text{S}_{1-x}\text{Se}_x)_2$  were obtained from the second derivative spectra of the dielectric function real and imaginary parts. Changes in the temperature dependences of critical point energies  $E_{cp}$  are observed at temperatures close to the phase transitions in  $\text{TlIn}(\text{S}_{1-x}\text{Se}_x)_2$ .

#### Acknowledgement

The first author gratefully acknowledges Deutscher Akademischer Austauschdienst (DAAD) for the financial support of his research stay at Technische Universität Chemnitz (project No. A/12/85971).

#### References

[1] A.M. Panich, Electronic properties and phase transitions in low-dimensional semiconductors, *J. Phys.: Condens. Matter* 20 (29) (2008) 293202, 1–42 (Topical Review).

[2] N.A. Abdullaev, K.R. Allakhverdiev, G.L. Belenku, T.G. Mamedov, R.A. Suleimanov, Ya.N. Sharifov, Phase transition and anisotropy of thermal expansion in  $\text{TlInS}_2$ , *Solid State Commun.* 53 (1985) 601–602.

[3] R. Laiho, T. Levola, R.M. Sardar, K.R. Allakhverdiev, I.Sh. Sadykov, M.M. Tagiev, Brillouin scattering study of phase transitions in  $\text{TlInS}_2$ , *Sol. State Commun.* 63 (1987) 1189–1192.

[4] M. Haniyas, A. Anagnostopoulos, K. Kambas, J. Spyridelis, On the non-linear properties of  $\text{TlInX}_2$  ( $X = \text{S}, \text{Se}, \text{Te}$ ) ternary compounds, *Physica B* 160 (1989) 154–160.

[5] K.R. Allakhverdiev, S.S. Babaev, N.M. Tagiev, M.M. Shirinov, Low-temperature IR and Raman scattering spectra of  $\text{TlInS}_2$  layered crystal, *Phys. Status Solidi B* 152 (1989) 317–327.

[6] V.M. Burlakov, A.P. Ryabov, M.P. Yakheev, E.A. Vinogradov, N.N. Melnik, N.M. Gasanly, Raman spectroscopy of soft and rigid modes in ferroelectric  $\text{TlInS}_2$ , *Phys. Status Solidi B* 153 (1989) 727–739.

[7] K.R. Allakhverdiev, N. Türetken, F.M. Salaev, F.A. Mikailov, Succession of the low temperature phase transitions in  $\text{TlInS}_2$  crystals, *Sol. State Commun.* 96 (1995) 827–831.

[8] S. Kashida, Y. Kobayashi, X-ray study of the incommensurate phase of  $\text{TlInS}_2$ , *J. Phys.: Condens. Matter* 11 (1999) 1027–1036.

[9] E. Senturk, L. Tumbek, F.A. Mikailov, F. Salehli, Dielectric relaxation in ferroelectric  $\text{TlInS}_2$  layered crystals within metastable chaotic state, *Cryst. Res. Technol.* 42 (2007) 626–630.

[10] N.A. Abdullaev, T.G. Mamedov, R.A. Suleimanov, Thermal expansion of single crystals of the layered compounds  $\text{TlGaSe}_2$  and  $\text{TlInS}_2$ , *Low Temp. Phys.* 27 (2001) 676–680.

[11] F.A. Mikailov, E. Basaran, T.G. Mammadov, M.Y. Seyidov, E. Senturk, R. Currat, Dielectric susceptibility behaviour in the incommensurate phase of  $\text{TlInS}_2$ , *Phys. B: Condens. Matter* 334 (2003) 13–20.

[12] A.F. Qasrawi, N.M. Gasanly, Photoelectronic, optical and electrical properties of  $\text{TlInS}_2$  single crystals, *Phys. Status Solidi A* 199 (2003) 277–283.

[13] Y.G. Shim, N. Uneme, S. Abdullayeva, N. Mamedov, N. Yamamoto, Light figure studies of optical anisotropy induced by nanoscale spatial modulation in  $\text{TlInS}_2$ , *J. Phys. Chem. Solids* 66 (2005) 2116–2118.

[14] A.F. Qasrawi, N.M. Gasanly, Optical properties of  $\text{TlInS}_2$  layered single crystals near the absorption edge, *J. Mater. Sci.* 41 (2006) 3569–3572.

[15] W. Henkel, H.D. Hochheimer, C. Carlone, A. Werner, S. Ves, H.G. v. Schnering, High-pressure raman study of the ternary chalcogenides  $\text{TlGaS}_2$ ,  $\text{TlGaSe}_2$ ,  $\text{TlInS}_2$ , and  $\text{TlInSe}_2$ , *Phys. Rev. B* 26 (1982) 3211–3221.

[16] K.R. Allakhverdiev, T.G. Mamedov, G.I. Peresada, E.G. Ponomarev, Ya.N. Sharifov, Phase diagrams of layered semiconductors  $\text{TlInS}_2$ ,  $\text{TlGaS}_2$ , and  $\text{TlGaSe}_2$  under hydrostatic pressures up to 1.2 GPa, *Sov. Phys. Solid State* 27 (1985) 568–569.

[17] E. Bairamova, K.R. Allakhverdiev, B.G. Akinoglu, T. Arai, T.G. Mamedov, Raman scattering in layer  $\text{TlIn}_x\text{Ga}_{1-x}\text{S}_2$  under pressure, *Turk. J. Phys.* 18 (1994) 497–506.

[18] O.O. Gomonnai, P.P. Guranich, M.Y. Rigan, I.Y. Roman, A.G. Slivka, Effect of hydrostatic pressure on phase transitions in ferroelectric  $\text{TlInS}_2$ , *High Press. Res.* 28 (2008) 615–619.

[19] P.P. Guranich, R.R. Rosul, O.O. Gomonnai, A.G. Slivka, I. Yu. Roman, A.V. Gomonnai, Ferroelasticity of  $\text{TlInS}_2$  crystal, *Solid State Commun.* 106 (2014) 21–24.

[20] N.M. Gasanly, H. Özkan, A. Çulfaz, Composition variations of lattice parameters of  $\text{TlIn}(\text{Se}_{1-x}\text{Te}_x)_2$ ,  $\text{TlIn}(\text{Se}_{1-x}\text{S}_x)_2$  and  $\text{TlIn}_{1-x}\text{Ga}_x\text{Se}_2$  mixed crystals, *Cryst. Res. Technol.* 30 (1995) 109–113.

[21] A.U. Sheleg, V.G. Hurtavy, V.V. Shautsova, V.A. Aliev, X-ray diffraction study of the crystallographic characteristics of  $\text{TlInS}_x\text{Se}_{2-x}$  solid solutions, *Crystallogr. Rep.* 59 (2014) 186–189.

[22] N.M. Gasanly, Influence of isomorphic atom substitution on lattice anisotropy of thallium dichalcogenide layered mixed crystals, *Acta Phys. Pol. A* 110 (2006) 471–477.

[23] M. Yu. Seyidov, R.A. Suleymanov, F. Salehli, Origin of structural instability in  $\text{TlInS}_{2(1-x)}\text{Se}_{2x}$  solid solutions, *Phys. Scr.* 84 (2011) 015601.

[24] E.A. Vinogradov, N.M. Gasanly, A.F. Goncharov, B.M. Dzhavadov, V.I. Tagirov, Structural phase transitions in thallium indium sulfide selenide ( $\text{TlInS}_2\text{Se}_{2(1-x)}$ ) and thallium gallium indium selenide ( $\text{TlGa}_x\text{In}_{1-x}\text{Se}_2$ ) solid solutions, *Sov. Phys. Solid State* 22 (1980) 526–527.

[25] K.R. Allakhverdiev, N.D. Akhmedzade, N.M. Tagiev, M.M. Shirinov, S. Häsel, Long-wavelength IR-active phonons in the  $\text{TlInS}_2$ – $\text{TlInSe}_2$  system, *Phys. Status Solidi B* 148 (1988) K93–K96.

[26] Sh. Nurov, V.M. Burlakov, E.A. Vinogradov, N.M. Gasanly, B.M. Dzhavadov, Vibration spectra of  $\text{TlInS}_2$ ,  $\text{TlIn}_{0.95}\text{Ga}_{0.05}\text{S}_2$  and  $\text{TlIn}(\text{S}_{0.8}\text{Se}_{0.2})_2$  crystals in the vicinity of phase transitions, *Phys. Status Solidi B* 137 (1986) 21–32.

[27] N.M. Gasanly, B.M. Dzhavadov, V.I. Tagirov, E.A. Vinogradov, Long-wave lattice vibrations of  $\text{TlInS}_{2x}\text{Se}_{2(1-x)}$  and  $\text{TlGaS}_{2x}\text{Se}_{2(1-x)}$  layered solid solutions, *Phys. Status Solidi B* 95 (1979) K27–K30.

[28] N.A. Bakhyshev, N.M. Gasanly, B.M. Yavadov, V.I. Tagirov, S.M. Efendiev, Mixed one- and two- mode behaviour of optical phonons in  $\text{TlGaS}_{2x}\text{Se}_{2(1-x)}$  and  $\text{TlInS}_{2x}\text{Se}_{2(1-x)}$  layered solid solutions, *Phys. Status Solidi B* 91 (1979) K1–K3.

[29] I. Guler, N.M. Gasanly, Raman scattering in  $\text{TlInS}_{2x}\text{Se}_{2(1-x)}$  layered mixed crystals ( $0.25 \leq x \leq 1$ ): compositional dependence of the mode frequencies and line widths, *Physica B* 406 (2011) 3374–3376.

[30] N.M. Gasanly, Effect of temperature and isomorphic atom substitution on optical absorption edge of  $\text{TlInS}_{2x}\text{Se}_{2(1-x)}$  mixed crystals ( $0.25 \leq x \leq 1$ ), *Cryst. Res. Technol.* 45 (2010) 525–528.

- [31] N.M. Gasanly, Band gap and refractive index tunability in thallium based layered mixed crystals, *J. Appl. Phys.* 118 (2015) 035701.
- [32] A.U. Sheleg, V.G. Hurtavy, V.V. Shautsova, V.A. Aliev, Dielectric properties and phase transitions in crystals of  $\text{TlInS}_x\text{Se}_{2-x}$  solid solutions, *Phys. Solid State* 54 (2012) 622–625.
- [33] R.R. Rosul, P.P. Guranich, O.O. Gomonnai, A.G. Slivka, M. Yu. Rigan, V.M. Rubish, O.G. Guranich, A.V. Gomonnai, Dielectric properties of  $\text{TlIn}(\text{S}_{1-x}\text{Se}_x)_2$  polycrystals near phase transitions, *Semicond. Phys. Quant. Electr. Optoelectr.* 15 (2012) 35–37.
- [34] A.V. Gomonnai, A.A. Grabar, Yu. M. Vysochanskii, A.D. Belyaev, V.F. Machulin, M.I. Gurzan, V. Yu. Slivka, The splitting of the phase transition in the ferroelectric solid solutions, *Fiz. Tverd. Tela* 23 (1981) 3602–3606.
- [35] M. Isik, N.M. Gasanly, R. Turan, Spectroscopic ellipsometry study of above-bandgap optical constants of layered structured  $\text{TlGaSe}_2$ ,  $\text{TlGaS}_2$  and  $\text{TlInS}_2$  single crystals, *Physica B* 407 (2012) 4193–4197.
- [36] T. Kawabata, Y.G. Shim, K. Wakita, N. Mamedov, Dielectric function spectra and inter-band optical transitions in  $\text{TlGaS}_2$ , *Thin Solid Films* 571 (2014) 589–592.
- [37] M. Isik, N.M. Gasanly, Ellipsometry study of interband transitions in  $\text{TlGaS}_{2x}\text{Se}_{2(1-x)}$  mixed crystals ( $0 \leq x \leq 1$ ), *Opt. Commun* 285 (2012) 4092–4096.
- [38] M. Isik, N.M. Gasanly, Interband critical points in  $\text{TlGa}_x\text{In}_{1-x}\text{S}_2$  mixed crystals ( $0 \leq x \leq 1$ ), *J. Alloys Compd.* 481 (2013) 542–546.
- [39] I. Guler, Optical analysis of  $\text{TlInS}_{2x}\text{Se}_{2(1-x)}$  mixed crystals, *J. Appl. Phys.* 115 (2014) 033517.
- [40] Y.G. Shim, T. Kawabata, K. Wakita, N. Mamedov, Temperature behavior of dielectric function spectra and optical transitions in  $\text{TlGaS}_2$ , *Phys. Status Solidi B* 252 (2015) 1254–1257.
- [41] N. Mamedov, Y. Shim, W. Okada, R. Tashiro, K. Wakita, Band gap exciton in ferroelectric  $\text{TlInS}_2$ : dimensionality and screening, *Phys. Status Solidi B* 252 (2015) 1248–1253.
- [42] A.V. Gomonnai, I. Petryshynets, Yu. M. Azhniuk, O.O. Gomonnai, Yu. I. Roman, I.I. Turok, A.M. Solomon, R.R. Rosul, D.R.T. Zahn, Growth and characterisation of sulphur-rich  $\text{TlIn}(\text{S}_{1-x}\text{Se}_x)_2$  single crystals, *J. Cryst. Growth* 367 (2013) 35–41.
- [43] H. Fujiwara, *Spectroscopic Ellipsometry Principles and Applications*, John Wiley & Sons, NewYork, 2007.
- [44] S. Adachi, *Optical Properties of Crystalline and Amorphous Semiconductors: Materials and Fundamental Principles*, Springer Science & Business Media, 2012.
- [45] A. Savitzky, M.J.E. Golay, Smoothing and differentiation of data by simplified least squares procedures, *Anal. Chem.* 36 (1964) 1627–1639.